



Article

# C-X-C Motif Chemokine Ligand 9 and Its CXCR3 Receptor Are the Salt and Pepper for T Cells Trafficking in a Mouse Model of Gaucher Disease

Albert Frank Magnusen <sup>1,†</sup>, Reena Rani <sup>2,†</sup>, Mary Ashley McKay <sup>1,†</sup> , Shelby Loraine Hatton <sup>1</sup>,  
Tsitsi Carol Nyamajenje <sup>1</sup>, Daniel Nii Aryee Magnusen <sup>1</sup>, Jörg Köhl <sup>3,4</sup> , Gregory Alex Grabowski <sup>5,6</sup>  
and Manoj Kumar Pandey <sup>6,\*</sup>

- <sup>1</sup> Division of Human Genetics, Cincinnati Children's Hospital Medical Center, 3333 Burnet Avenue, Cincinnati, OH 45229, USA; albert.magnusen@cchmc.org (A.F.M.); Mary\_McKay@rush.edu (M.A.M.); shelby.hatton@cchmc.org (S.L.H.); nyamajtc@mail.uc.edu (T.C.N.); daniel.magnusen@sinclair.edu (D.N.A.M.)
- <sup>2</sup> Division of Immunobiology, Cincinnati Children's Hospital Medical Center, 3333 Burnet Avenue, Cincinnati, OH 45229, USA; reenacchmc@gmail.com
- <sup>3</sup> Institute for Systemic Inflammation Research, University of Lübeck, 23562 Lübeck, Germany; joerg.koehl@uksh.de
- <sup>4</sup> Department of Pediatrics and Division of Immunobiology, Cincinnati Children's Hospital Medical Center, College of Medicine, University of Cincinnati, 3333 Burnet Avenue, Cincinnati, OH 45229, USA
- <sup>5</sup> Department of Molecular Genetics, Biochemistry and Microbiology, Division of Human Genetics, Cincinnati Children's Hospital Medical Center, College of Medicine, University of Cincinnati, 3333 Burnet Avenue, Cincinnati, OH 45229, USA; grabgo317@comcast.net
- <sup>6</sup> Department of Pediatrics, Division of Human Genetics, Cincinnati Children's Hospital Medical Center, College of Medicine, University of Cincinnati, 3333 Burnet Avenue, Cincinnati, OH 45229, USA
- \* Correspondence: manoj.pandey@cchmc.org
- † These authors contributed equally to this work.



**Citation:** Magnusen, A.F.; Rani, R.; McKay, M.A.; Hatton, S.L.; Nyamajenje, T.C.; Magnusen, D.N.A.; Köhl, J.; Grabowski, G.A.; Pandey, M.K. C-X-C Motif

Chemokine Ligand 9 and Its CXCR3 Receptor Are the Salt and Pepper for T Cells Trafficking in a Mouse Model of Gaucher Disease. *Int. J. Mol. Sci.* **2021**, *22*, 12712. <https://doi.org/10.3390/ijms222312712>

Academic Editors: Burkhard Kleuser, Elisabetta Meacci and Shunji Tomatsu

Received: 1 August 2021

Accepted: 18 November 2021

Published: 24 November 2021

**Publisher's Note:** MDPI stays neutral with regard to jurisdictional claims in published maps and institutional affiliations.



**Copyright:** © 2021 by the authors. Licensee MDPI, Basel, Switzerland. This article is an open access article distributed under the terms and conditions of the Creative Commons Attribution (CC BY) license (<https://creativecommons.org/licenses/by/4.0/>).

**Abstract:** Gaucher disease is a lysosomal storage disease, which happens due to mutations in *GBA1/Gba1* that encodes the enzyme termed as lysosomal acid  $\beta$ -glucosidase. The major function of this enzyme is to catalyze glucosylceramide (GC) into glucose and ceramide. The deficiency of this enzyme and resultant abnormal accumulation of GC cause altered function of several of the innate and adaptive immune cells. For example, augmented infiltration of T cells contributes to the increased production of pro-inflammatory cytokines, (e.g., IFN $\gamma$ , TNF $\alpha$ , IL6, IL12p40, IL12p70, IL23, and IL17A/F). This leads to tissue damage in a genetic mouse model (*Gba1*<sup>9V/-</sup>) of Gaucher disease. The cellular mechanism(s) by which increased tissue infiltration of T cells occurs in this disease is not fully understood. Here, we delineate role of the CXCR3 receptor and its exogenous C-X-C motif chemokine ligand 9 (CXCL9) in induction of increased tissue recruitment of CD4<sup>+</sup> T and CD8<sup>+</sup> T cells in Gaucher disease. Intracellular FACS staining of macrophages (M $\phi$ s) and dendritic cells (DCs) from *Gba1*<sup>9V/-</sup> mice showed elevated production of CXCL9. Purified CD4<sup>+</sup> T cells and the CD8<sup>+</sup> T cells from *Gba1*<sup>9V/-</sup> mice showed increased expression of CXCR3. Ex vivo and in vivo chemotaxis experiments showed CXCL9 involvement in the recruitment of *Gba1*<sup>9V/-</sup> T cells. Furthermore, antibody blockade of the CXCL9 receptor (CXCR3) on T cells caused marked reduction in CXCL9-mediated chemotaxis of T cells in *Gba1*<sup>9V/-</sup> mice. These data implicate abnormalities of the CXCL9-CXCR3 axis leading to enhanced tissue recruitment of T cells in Gaucher disease. Such results provide a rationale for blockade of the CXCL9/CXCR3 axis as potential new therapeutic targets for the treatment of inflammation in Gaucher disease.

**Keywords:** lysosomal storage disease; chemokine; chemokine receptor; inflammation

## 1. Introduction

Gaucher disease (GD) is a lysosomal storage disorder with a worldwide incidence of approximately 1/40,000 to 1/100,000 [1,2]. GD is caused by *GBA1* mutations that

lead to decreased activity of lysosomal acid  $\beta$ -glucosidase (D-glucosyl-N-acylsphingosine glucosylceramide (GC) [3,4]. Macrophage (M $\phi$ ) lineage cells are prominent disease effectors due to their massive accumulation of GC, i.e., Gaucher cells. This leads to their secretion of numerous cytokines and chemokines that influence other innate and adaptive immune cells [5–8]. The resultant tissue manifestations of GD lead to the clinical signs of anemia, thrombocytopenia, hypergammaglobulinemia, splenomegaly, hepatomegaly, bone, and brain defects) [1,6,9–14]. Many of these signs are recapitulated in a genetic GD-mouse model (D409 V/null; 9 V/null; *Gba1*<sup>9V/-</sup>) including, tissue accumulation of Gaucher cells and GC in lung, liver, and spleen as well as infiltration of T cells [4,5,13,15–22].

T lymphocytes are the major effector cells in cellular immunity and produce cytokines in response to variety of antigens, which leads to inflammation in several diseases [23–27]. Two major groups T cells are termed CD4<sup>+</sup> T-helper and CD8<sup>+</sup> T cytotoxic cells [28]. CD4<sup>+</sup> T helper cells showed significant heterogeneity of their cytokine expression profiles that lead to the discoveries of interferon gamma (IFN $\gamma$ ) producing T helper 1 (Th1), interleukin (IL) 4 producing Th2, and IL17 producing Th17 cell subsets [26,29,30]. This cytokine heterogeneity specifies the interaction of T cells with other immune cells and thereby their function in host defense and inflammation [25,31–36]. CD8<sup>+</sup> T cells are important for inducing autoimmune and the anti-cancer and anti-viral responses [37–40]. T cell defects, T cell lymphomas, and increased incidence of CD3<sup>+</sup>, CD4<sup>+</sup>, CD8<sup>+</sup>, CD3<sup>+</sup>HLA-DR<sup>+</sup>, CD4<sup>+</sup>HLA-DR<sup>+</sup>, and CD8<sup>+</sup>HLA-DR<sup>+</sup> subset of activated T cells have been observed in lung and peripheral blood of patients with GD [41–46]. Significantly elevated levels of CD4<sup>+</sup> T cells and modest changes in CD8<sup>+</sup> T cells were present in liver, lung, spleen, and thymus of *Gba1*<sup>9V/-</sup> mice [5,6,47]. The CD3/CD28-mediated GC-dependent activation of liver-, lung-, and spleen-derived T cells in co-culture of DC and CD4<sup>+</sup> T cells have shown increased production of several of the pro-inflammatory cytokines, i.e., IFN $\gamma$ , tumor necrosis factor alpha (TNF $\alpha$ ), IL6, IL12p40, IL12p70, IL23, and IL17A/F. This pro-inflammatory environment leads to the tissue damage in *Gba1*<sup>9V/-</sup> GD mouse model. The genetic deficiency or pharmaceutical blockade of complement 5a (C5a) receptor 1 (C5aR1) resulted in reduction of activated subsets of CD4<sup>+</sup> T cells as well as the decreased generation of pro-inflammatory cytokines in co-cultured cells, (e.g., DC and CD4<sup>+</sup> T cells) from *Gba1*<sup>9V/-</sup> mice [16]. However, the exact cellular mechanism(s) that causes enhanced tissue recruitment of T cells in *Gba1*<sup>9V/-</sup> mice is still unclear.

C-X-C motif ligand 9 (CXCL9), CXCL10, and CXCL11 belong to the CXC subfamily of chemokines. These are induced by IFN $\gamma$  and are crucial for recruitment of T cells and other immune cell phenotypes, (e.g., NK cells) to the sites of inflammation, due to their binding to chemokine receptor CXCR3 [48–60]. CXCR3 is the member of G protein coupled receptor family and is expressed on different subsets of T cells [61–64]. IFN $\gamma$  drives increased expression of CXCR3 and its ligands, (e.g., CXCL9–11) that are increased in several inflammatory diseases [64–70]. Elevated levels of IFN $\gamma$  and CXCL9–11 as well as increased numbers of tissue T cells were found in GD mouse models and human patients with GD [5,6,15,41–45,47,71]. However, the cellular mechanism(s) that causes increased tissue recruitment of T cells in *Gba1*<sup>9V/-</sup> mice is unclear. Here, analyses of CXCL9-mediated ex vivo and in vivo T cells chemotaxis in the presence or absence of mouse anti-CXCR3 antibodies identified a role of the CXCL9-CXCR3 axis in excess trafficking of T cells into tissues affected by GD.

## 2. Materials and Methods

### 2.1. Materials

The following reagents were from BD Biosciences (San Jose, CA, USA) or eBiosciences (San Diego, CA, USA): Monoclonal antibodies to CD11b-FITC (M1/70), F4/80-PerCP5.5, CD11c-APC, CD3-pacific blue, CD4-FITC, CD8-APC, CXCL9-PE, CXCR3/CD183-PE and their corresponding isotype antibodies (Rat IgG2a-FITC, Rat IgG2a-PerCP5.5, Armenian hamster IgG-APC, Rat IgG2a-pacific blue, Rat IgG2a-FITC, Rat IgG2a APC, Hamster IgG-

PE). Recombinant murine CXCL9 from Pepro Tech (Cranbury, NJ, USA) and purified mouse anti-CXCR3 antibodies (catalog number-155902, clone-S18001A, and lot number-B265189) was from Biolegend (San Diego, CA, USA). Liberase CI was from Roche (Indianapolis, IN, USA). Bovine serum albumin (BSA), Gey's balanced salt solution (GBSS), and DNase were from Sigma (St. Louis, MO, USA). Anti-CD11b, CD11c, CD4, and CD8 microbeads were from Miltenyi Biotec (Auburn, CA, USA). Diff-Quik stain set was from Dade Behring, Inc. (Newark, NJ, USA). Polycarbonate membranes, cell scraper, and Boyden chemotaxis chamber were from Neuro Probe, Inc. (Gaithersburg, MD, USA). ELISA kit for the detection of mouse CXCL9 was from R&D System (Minneapolis, MN, USA). LSRII flow cytometer from BD Biosciences (San Jose, CA, USA), FCS Express software from De Novo Software (Los Angeles, CA, USA).

## 2.2. Mice

The D409 V/null mice (9 V/null; *Gba1<sup>9V/-</sup>*) and WT control were of the mixed background FVB/C57BL/6J/129SvEvBrd (50:25:25) [4] and were 12 weeks of age. The new nomenclature for D409V includes the 39 amino acid leader sequence and would then be Asp448Val or p.D448V. Mice were maintained under pathogen-free conditions. All mice were housed under pathogen-free conditions in the barrier animal facility according to IACUC-approved protocol (IACUC2020-0052) at Cincinnati Children's Hospital Research Foundation (CCHRF).

## 2.3. Cell Preparation

Lung, spleen, blood, and peritoneal lavage from WT and *Gba1<sup>9V/-</sup>* mice were removed aseptically. Single cell suspensions prepared from lung were obtained from minced pieces that were treated with Liberase CI (0.5 mg/mL) and DNase (0.5 mg/mL) in RPMI (45 min, 37 °C) and spleen by direct grinding. Blood mononuclear cells were obtained after red blood cell (RBC) lysis (155 mM NH<sub>4</sub>Cl, 10 mM NaHCO<sub>3</sub>, 0.1 mM EDTA). Single cell suspensions prepared from lung, spleen, and the peritoneal lavage were filtered through a 70-micron cell strainer followed by RBC lysis, passage through a strainer, and pelleted by centrifugation at 350 g. Viable cells were counted using a Neubauer chamber and trypan blue exclusion. Mφs, DCs, CD4<sup>+</sup> T lymphocytes, and CD8<sup>+</sup> T lymphocytes were purified from single cell suspensions of lung and spleen using CD11c, CD11b, CD4 (L3T4), and CD8a (Ly2) microbeads according to the manufacturer's protocol.

## 2.4. Flow Cytometry

FACS staining was performed for characterization of immunological cell types in lung, spleen, blood, and peritoneal lavage and the chemotactic cells obtained after their migration. These cells were washed with PBS containing 1% BSA. After incubation for 15 min at 4 °C with the blocking antibody 2.4G2 (anti-FcγRII and III), all cells were stained at 4 °C for 45 min with the appropriate labeled antibodies for different cell types, i.e., anti-mouse CD11b and anti-mouse F4/80 antibodies for Mφs, anti-mouse CD11b, anti-mouse CD11c antibodies for DCs, anti-mouse CD3, CD4, and CD8, antibodies for T cells, and anti-mouse B220 antibodies for B cells. In separate batches, the cells were stained with the respective isotypes. Flow cytometric analyses were performed, where Mφs were gated first by their typical FSC/SSC pattern based on monocyte gated cells and their F4/80 positivity and double stained for F4/80 and CD11b. For DCs, monocyte gated cells from FSC/SSC pattern were gated for CD11c positivity and double stained for CD11c and CD11b. Purified Mφs and DCs were used to perform intracellular cytokine staining for CXCL9 and its isotype, (e.g., Armenian Hamster IgG). Flow cytometric analyses of T lymphocytes were generated after gating lymphocytes from forward and side scatter and then identifying the CD3<sup>+</sup>, B220<sup>-</sup>CD3<sup>+</sup>CD4<sup>+</sup>, and B220<sup>-</sup>CD3<sup>+</sup>CD8<sup>+</sup> T lymphocytes. Mononuclear cells prepared from blood as well as purified CD4<sup>+</sup> T and CD8<sup>+</sup> T cells were used to perform surface staining for CXCR3 and its isotype, (e.g., Armenian Hamster IgG). In an addition

experiment, purified CD4<sup>+</sup> T cells and CD8<sup>+</sup> T cells were used for chemotaxis assays. Flow cytometric analyses were performed on a LSR II, and FCS Express software.

### 2.5. T Cell Chemotaxis

CD4<sup>+</sup> T cells prepared from spleen of WT and *Gba1*<sup>9V/-</sup> mice were suspended in chemotaxis medium (GBSS containing 2% BSA) at a density of  $5 \times 10^6$  cells/mL. The different concentration of CXCL9, (e.g., 0, 2, 4, 8, 16, and 32 nM) in chemotaxis medium, placed in the bottom wells of a micro-Boyden chambers and overlaid with a 3  $\mu$ m polycarbonate membrane. Then, 50  $\mu$ L of the cells were placed in the top wells and incubated for 45 min at 37 °C. Subsequently, the membranes were removed and the cells on the bottom side of the membrane were stained with Diff-Quick. The numbers of migrated cells in five high-power fields were counted and the number of cells per mm<sup>2</sup> was calculated by computer assisted light microscopy. Results are expressed as the mean value of triplicate samples.

### 2.6. Ex Vivo Blocking of CXCR3 and T Cells Chemotaxis

To examine whether ex vivo blocking of CXCR3 using mouse anti-CXCR3 antibodies can reduce CXCL9 mediated chemotaxis of T cell subsets in *Gba1*<sup>9V/-</sup> GD model, spleen-derived CD4<sup>+</sup> T cells and CD8<sup>+</sup> T cells ( $5 \times 10^6$  cells/mL) prepared from WT and *Gba1*<sup>9V/-</sup> mice were treated in the presence and absence of antibodies to mouse CXCR3 (10  $\mu$ g/mL) at 4 °C for 30 min. These cells were applied to subsequent top wells of Boyden chemotaxis chamber and chemotaxis was performed towards CXCL9 (16 nM) at 37 °C and 5% CO<sub>2</sub> for 45 min. The membrane was removed, and cells were scraped off using a vertical glass slide on the top of 50 mL falcon tube. These cells were stained with antibodies to specific cell phenotypes as discussed above.

### 2.7. In Vivo Blocking of CXCR3 and T Cells Chemotaxis

To examine whether in vivo blocking of CXCR3 alters CXCL9-mediated increased tissue recruitment of T cells in Gaucher disease, WT ( $n = 5$ ) and *Gba1*<sup>9V/-</sup> mice ( $n = 5$ ) were injected intraperitoneally (IP) with CXCL9 (200 nM:100  $\mu$ L) and their vehicle (PBS). In some experiments, mice were pretreated intravenously (IV) with mouse anti-CXCR3 antibodies (1.0 mg/kg body weight) prior to IP injections of CXCL9 or vehicle (PBS). After 6 h, mice were killed, and the peritoneal cavity was lavage with 10 mL of PBS. Peritoneal cells were washed once with PBS, and  $10^5$  cells in 200  $\mu$ L of PBS were used for performing FACS staining with antibodies to mouse CD3, CD4, and CD8s.

### 2.8. Determination of CXCL9 Production

M $\phi$ s and DCs purified from lung of the strain-matched *Gba1*<sup>9V/-</sup> and WT mice were cultured ( $10^6$  cells/200  $\mu$ L of complete RPMI media) for 48 h. CXCL9 concentrations were determined in the cell supernatants by commercial ELISA kits according to the manufacturer's instructions.

### 2.9. Statistical Analyses

Statistical significance was assessed by either one-tailed Students t-test (two groups) or analysis of variance (ANOVA) for multiple groups to determine significance performed using Prism Graph Pad™. Values shown in one asterisk (\*,  $p < 0.05$ ); two asterisks (\*\*,  $p < 0.01$ ); three asterisks (\*\*\*,  $p < 0.001$ ), and four asterisks (\*\*\*\*,  $p < 0.0001$ ) were considered statistically significant.

## 3. Results

### 3.1. *Gba1*<sup>9V/-</sup> Mice Immune Phagocytes Show Increased Levels of CXCL9 Chemokines

M $\phi$ s and DCs purified from lungs of WT and *Gba1*<sup>9V/-</sup> mice were used to assay CXCL9 chemokine levels. Compared to WT mouse M $\phi$ s, *Gba1*<sup>9V/-</sup> mouse M $\phi$ s had significantly increased amounts of CXCL9 (Figure 1a–e;  $p < 0.0001$ ). Similarly, as compared

to WT mice, *Gba1*<sup>9V/-</sup> mouse DCs showed significantly increased amounts of CXCL9 (Figure 1f–j;  $p < 0.0001$ ).

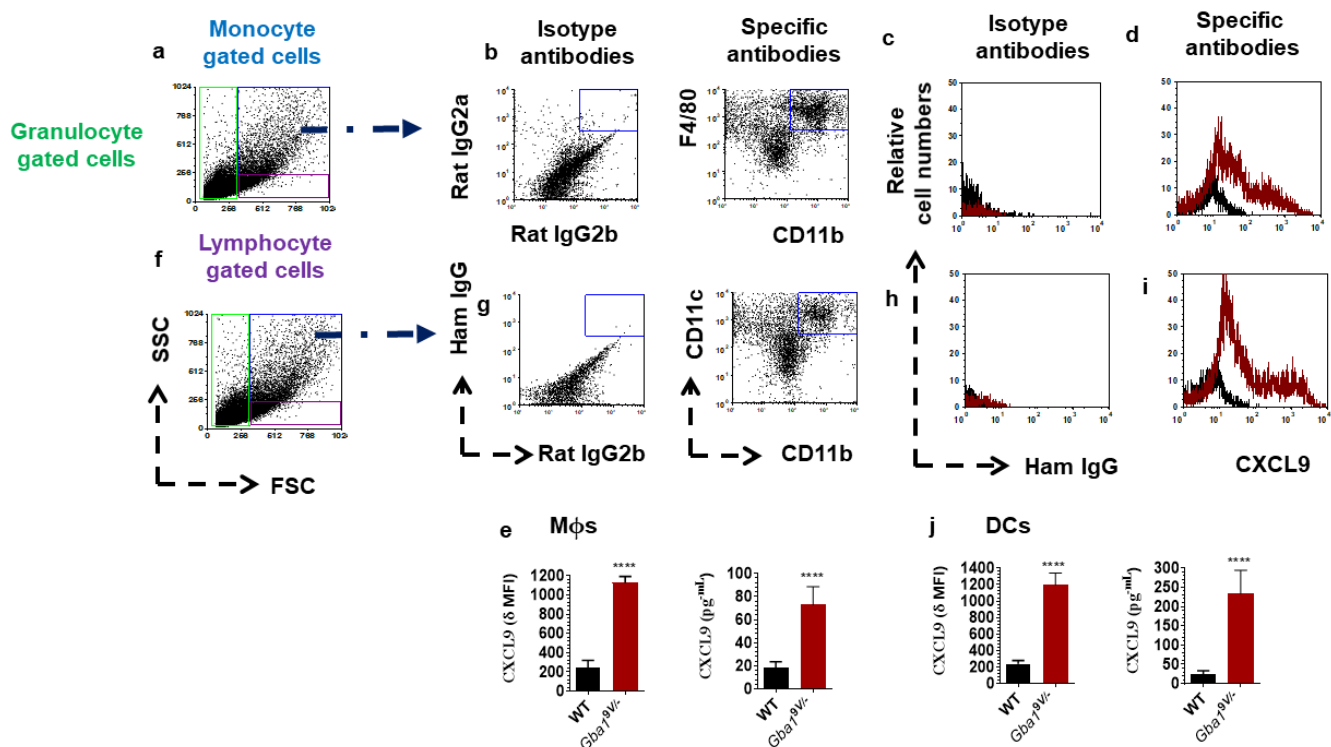


**Figure 1.** Immune phagocytes that cause increased amounts of CXCL9 in *Gba1*<sup>9V/-</sup> mouse tissues. CXCL9 amounts in monocyte gated F4/80<sup>hi</sup>CD11b<sup>+</sup> Mφs (a–e) and CD11c<sup>hi</sup>CD11b<sup>+</sup> DCs (f–j) from lung of strain-matched *Gba1*<sup>9V/-</sup> and WT mice ( $n = 5$ /group). Delta Mean Fluorescence Intensity ( $\delta$  MFI): CXCL9 MFI—*isotype* MFI. In the histograms of isotypes (c–h), specific antibodies (d–i), and the bar diagrams, the black lines/columns correspond to WT and the maroon lines/columns to *Gba1*<sup>9V/-</sup> cell. Values in d–h are the means  $\pm$  SD, and asterisks show significant differences between WT and *Gba1*<sup>9V/-</sup> mice (\*\*\*\*  $p < 0.0001$ ). Three independent experiments were conducted, and groups were compared using student's *t*-tests.

### 3.2. Identification of CXCR3 Positive T Cells in *Gba1*<sup>9V/-</sup> Mice

The single cell suspensions prepared from blood of WT and *Gba1*<sup>9V/-</sup> mice were analyzed for CXCR3<sup>+</sup>CD3<sup>+</sup> T cells. Compared to WT mouse samples, those from *Gba1*<sup>9V/-</sup> mice CD3<sup>+</sup> T cells had elevated amounts of CXCR3 (Supplementary Figure S1a–d;  $p < 0.0001$ ). An additional experiment CD4<sup>+</sup> T cells and CD8<sup>+</sup> T cells purified from lung of WT and *Gba1*<sup>9V/-</sup> mice were analyzed for CXCR3. Compared to WT mice, *Gba1*<sup>9V/-</sup> mouse CD4<sup>+</sup> T cells had elevated CXCR3 (Figure 2a–d;  $p < 0.0001$ ). In addition, as compared to WT, *Gba1*<sup>9V/-</sup> mouse CD8<sup>+</sup> T cells had elevated CXCR3 (Figure 2e–h;  $p < 0.0001$ ).

### 3.3. Effect of CXCL9 in Ex Vivo Chemotaxis of T Cells in *Gba1*<sup>9V/-</sup> Mice

*Gba1*<sup>9V/-</sup> mice immune phagocytes, (e.g., Mφs and DCs) showed increased amounts of CXCL9 and their receptor CXCR3 on T cell subsets when compared to WT. These data suggested a potential role of the CXCL9—CXCR3 pathway for increased numbers of T cells in *Gba1*<sup>9V/-</sup> mouse tissues. To confirm this, several concentrations of CXCL9 (0, 2, 4, 8, and 16 nM) were used to generate dose response curves for ex vivo chemotaxis of WT and *Gba1*<sup>9V/-</sup> mouse spleen-derived CD4<sup>+</sup> T cells. CXCL9 caused dose-dependent increase in chemotaxis of CD4<sup>+</sup> T cells in WT and *Gba1*<sup>9V/-</sup> mice; compared to WT, such effects were more pronounced in *Gba1*<sup>9V/-</sup> mice (Figure 3a–c;  $p < 0.01$ ;  $p < 0.0001$ ).

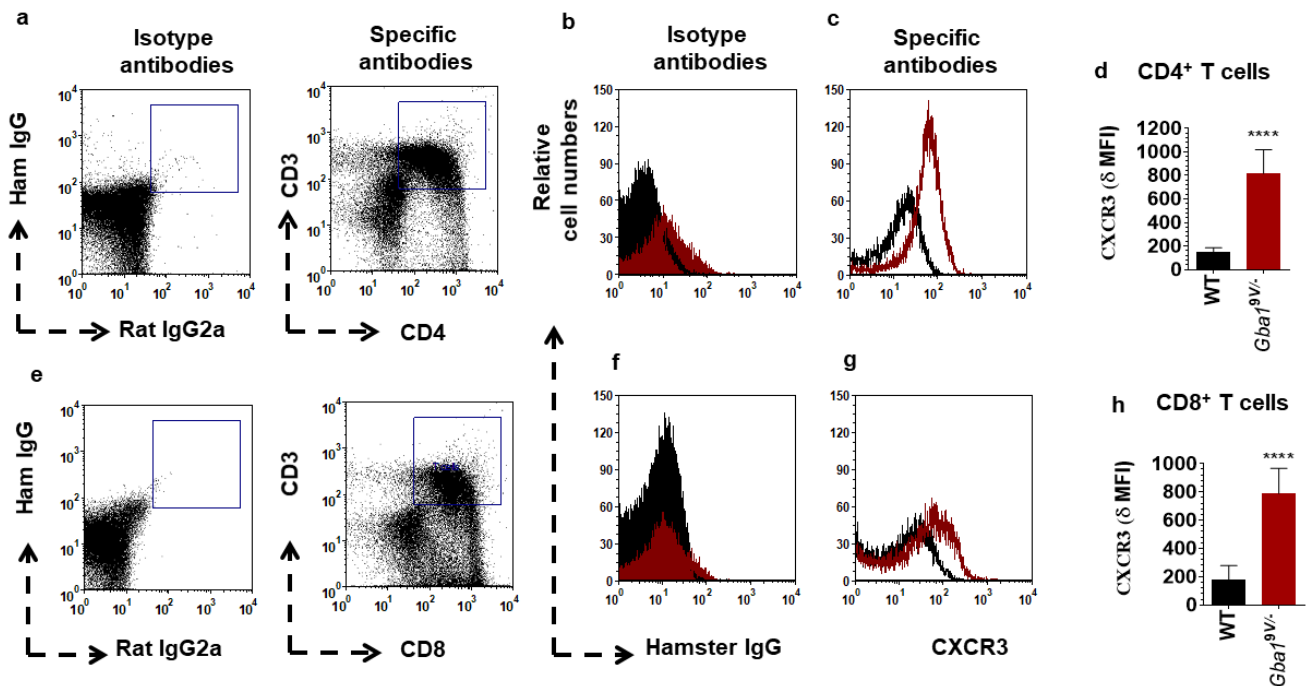


**Figure 2.** CXCR3 surface expression in pulmonary T cell subsets from *Gba1<sup>9V/-</sup>* mice. CXCR3 expression in FACS-sorted CD3<sup>+</sup>CD4<sup>+</sup> T cells (a–d) and CD3<sup>+</sup>CD8<sup>+</sup> T cells (e–h) from lung of strain-matched *Gba1<sup>9V/-</sup>* and WT mice (*n* = 5/group).  $\delta$  MFI: CXCR3 MFI—*isotype* MFI. In the dot plots of isotypes and specific antibodies (a,e), in the histograms of isotypes (b,f), specific antibodies (c,g), and the bar diagrams (d,h), the black lines/columns correspond to WT and the maroon lines/columns to *Gba1<sup>9V/-</sup>* mice. Values in d and h are the means  $\pm$  SD, and asterisks show significant differences between WT and *Gba1<sup>9V/-</sup>* mice (\*\*\*\* *p* < 0.0001). Three independent experiments were conducted, and groups were compared using student’s *t*-tests.

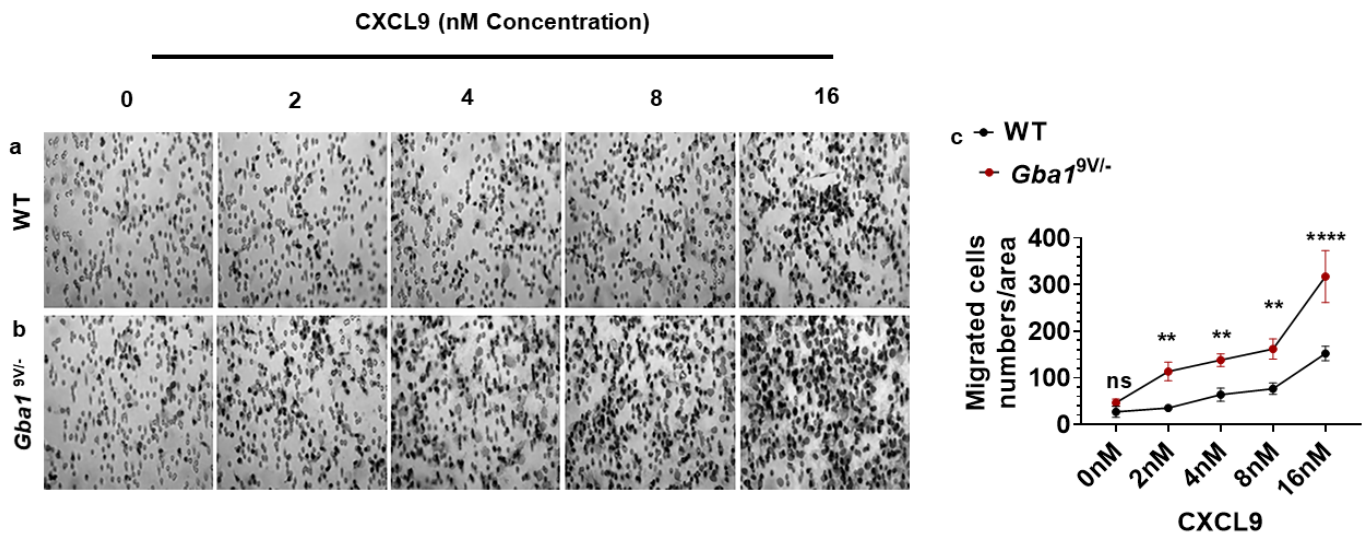


**Figure 3.** CXCL9 drives dose-dependent increased chemotaxis of T cell subsets in *Gba1<sup>9V/-</sup>* mice. Spleen-derived CD4<sup>+</sup> T cells from WT and *Gba1<sup>9V/-</sup>* mice (*n* = 5/group) were allowed to migrate towards different concentrations of CXCL9 (0, 2, 4, 8, and 16 nM) at 37 °C and 5% CO<sub>2</sub> for 45 min. The migration membrane was removed and stained with Diff-Quick and cells were counted under the light microscope. Diff quick- images and the corresponding bar diagrams represent the CXCL9 induced T cells migration in WT (a–c) and *Gba1<sup>9V/-</sup>* mice (b,c). WT (black curve), *Gba1<sup>9V/-</sup>* (maroon curve) and values shown are the mean  $\pm$  SD, and group comparison were performed with ANOVA (ns, not significant; \*\*, *p* < 0.01; \*\*\*\*, *p* < 0.0001).

### 3.4. Pharmaceutical Targeting of CXCR3 Leads to the Reduction of CXCL9 Mediated Ex Vivo T Cells Chemotaxis in *Gba1*<sup>9V/-</sup> Mice

Pharmaceutical blocking of CXCR3 confirmed the altered CXCL9-mediated ex vivo T cell chemotaxis in *Gba1*<sup>9V/-</sup> mice. Mouse anti-CXCR3 antibodies or vehicle (PBS) treated WT and *Gba1*<sup>9V/-</sup> mouse spleen-derived CD4<sup>+</sup> T cells were used for assessing their chemotaxis towards CXCL9 (Figure 4a–d). Similarly, mouse anti-CXCR3 antibodies or vehicle (PBS) treated WT and *Gba1*<sup>9V/-</sup> mouse spleen-derived CD8<sup>+</sup> T cells were used for assessing their chemotaxis towards CXCL9 (Figure 5a–d).

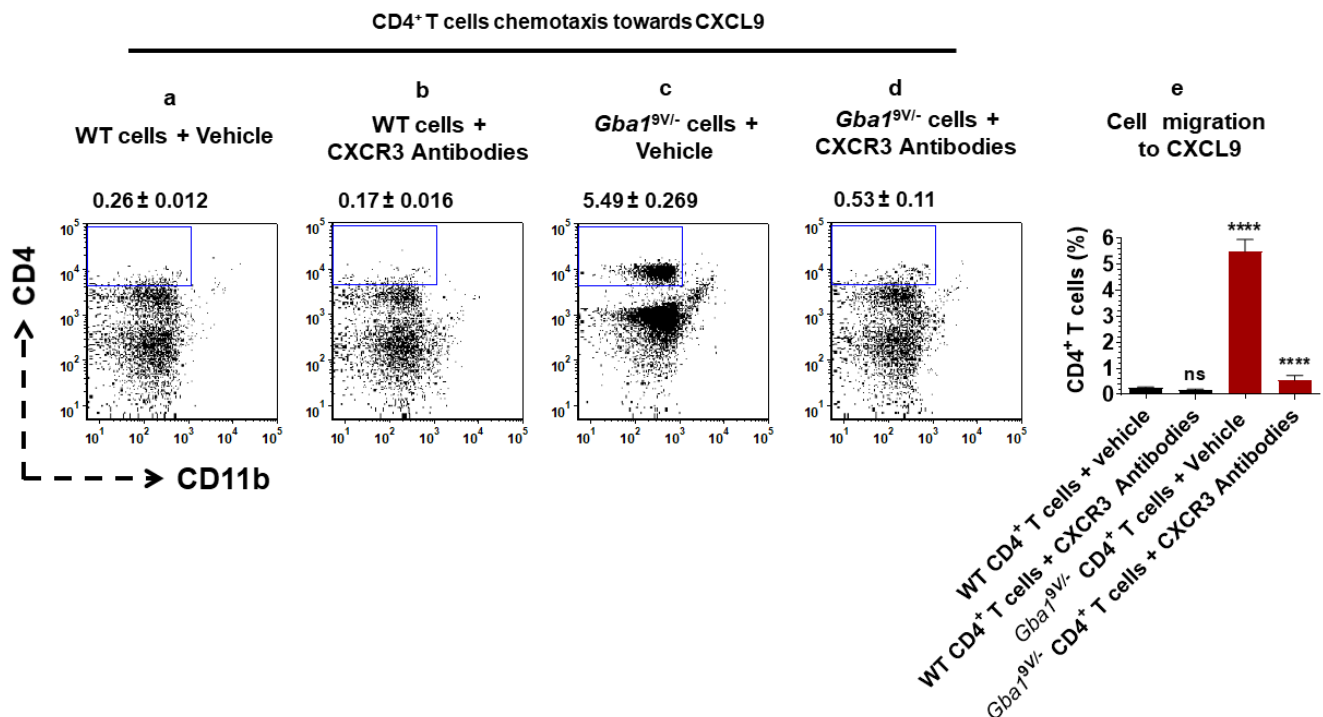


**Figure 4.** CXCR3 targeting alters CXCL9-mediated CD4<sup>+</sup> T cells chemotaxis in *Gba1*<sup>9V/-</sup> mice. CD4<sup>+</sup> T cells purified from spleen of WT and *Gba1*<sup>9V/-</sup> mice ( $n = 5$ /group) were allowed to migrate towards CXCL9 (16 nM) in the presence and absence of mouse anti-CXCR3 antibodies (10  $\mu$ g/mL) at 37 °C and 5% CO<sub>2</sub> for 45 min. Cells that had migrated through the filter and had attached to the lower side of the filter were collected and analyzed by FACS. Percentage of CD4<sup>+</sup>CD11b<sup>-</sup> T cells are shown from the (a) vehicle (PBS) treated WT cells and their migration to CXCL9, (b) mouse anti-CXCR3 antibodies treated WT cells and their migration to CXCL9, (c) PBS treated *Gba1*<sup>9V/-</sup> cells and their migration to CXCL9, and (d) mouse anti-CXCR3 antibodies treated *Gba1*<sup>9V/-</sup> cells and their migration to CXCL9. (e) WT (black columns), *Gba1*<sup>9V/-</sup> (maroon columns) and the values shown in the bar diagram are the mean  $\pm$  SD. and group comparison were performed with ANOVA. Three independent experiments were conducted (\*\*\*\*  $p < 0.0001$ ).

In additional experiments, anti-CXCR3 antibodies and vehicle (PBS) were used to treat WT and *Gba1*<sup>9V/-</sup> mice spleen-derived CD4<sup>+</sup> T and CD8<sup>+</sup> T cells. These CD4<sup>+</sup> T cells.

(Supplementary Figure S2a–e) and CD8<sup>+</sup> T cells (Supplementary Figure S3a–e) were used for chemotaxis quantification towards the corresponding chemotaxis buffer, i.e., 2% BSA-GBSS.

Cells were separated and analyzed by flow cytometry. Compared to WT, analyses of cells from *Gba1*<sup>9V/-</sup> mice that migrated towards CXCL9 showed increased percentages of CD4<sup>+</sup>CD11b<sup>-</sup> (Figure 4a,c,e;  $p < 0.0001$ ) and CD8<sup>+</sup>CD11b<sup>-</sup> T cells (Figure 5 a,c,e;  $p < 0.0001$ ). As compared to vehicle treated *Gba1*<sup>9V/-</sup> cells, mouse anti-CXCR3 antibodies treated *Gba1*<sup>9V/-</sup> cells showed reduction in CXCL9 mediated increased chemotaxis of CD4<sup>+</sup>CD11b<sup>-</sup> (Figure 4c–e;  $p < 0.0001$ ) and CD8<sup>+</sup>CD11b<sup>-</sup> T cells (Figure 5c–e;  $p < 0.0001$ ). However, these differences were not significant when compared to vehicle or mouse anti-CXCR3 antibodies treated WT CD4<sup>+</sup>CD11b<sup>-</sup> (Figure 4a,b,e; ns) or WT CD8<sup>+</sup>CD11b<sup>-</sup> T

cells (Figure 5a,b,e; ns). Furthermore, vehicle or mouse anti-CXCR3 antibodies treated WT and *Gba1*<sup>9V/-</sup> mouse CD4<sup>+</sup>CD11b<sup>-</sup>T (Supplementary Figure S2a–e; ns) or CD8<sup>+</sup>CD11b<sup>-</sup>T (Supplementary Figure S3a–e; ns) cells migration towards chemotaxis buffer did not differ.

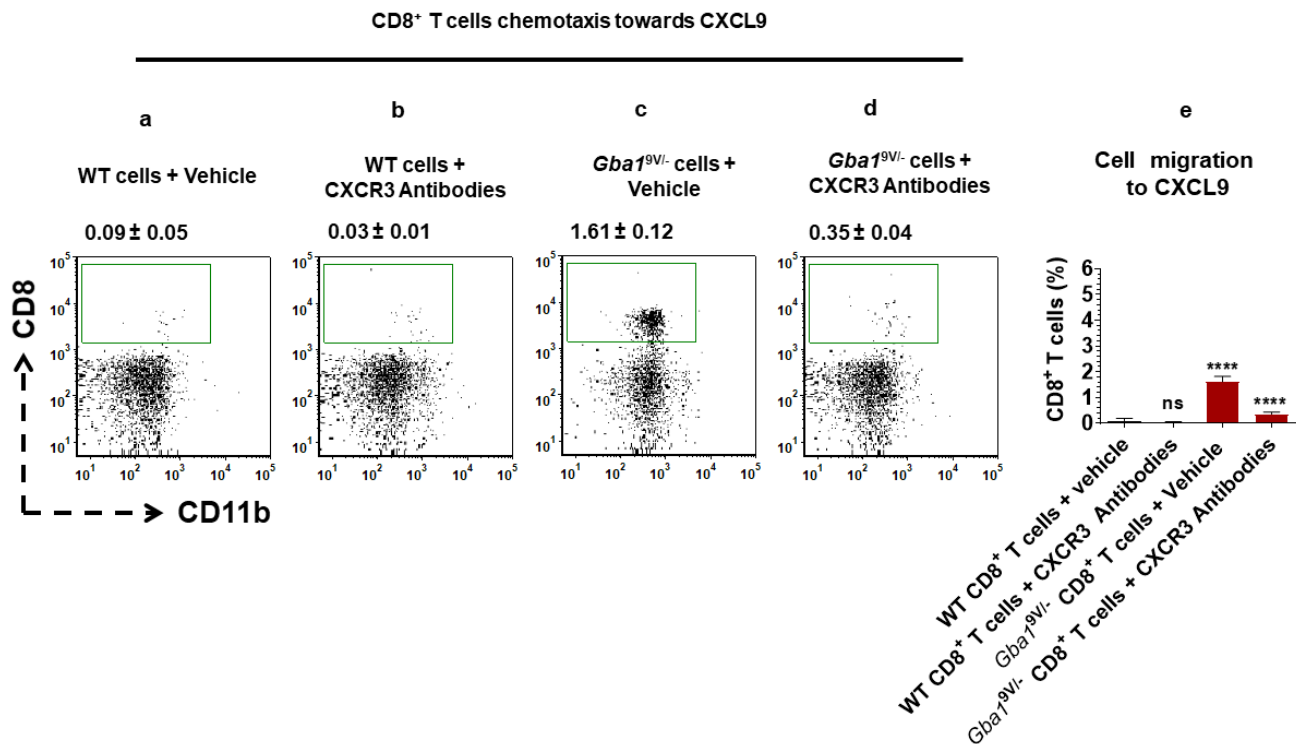


**Figure 5.** CXCR3 targeting alters CXCL9-mediated CD8<sup>+</sup> T cells chemotaxis in *Gba1*<sup>9V/-</sup> mice. CD8<sup>+</sup> T cells purified from spleens of WT and *Gba1*<sup>9V/-</sup> mice ( $n = 5/\text{group}$ ) were allowed to migrate towards CXCL9 (16 nM) in the presence and absence of mouse anti-CXCR3 antibodies (10  $\mu\text{g}/\text{mL}$ ) at 37 °C and 5% CO<sub>2</sub> for 45 min. Cells that had migrated through the filter and had attached to the lower side of the filter were collected and analyzed by FACS. Percentage of CD8<sup>+</sup>CD11b<sup>-</sup> T cells are shown from the (a) vehicle (PBS) treated WT cells and their migration to CXCL9, (b) mouse anti-CXCR3 antibodies treated WT cells and their migration to CXCL9, (c) PBS treated *Gba1*<sup>9V/-</sup> cells and their migration to CXCL9, and (d) mouse anti-CXCR3 antibodies treated *Gba1*<sup>9V/-</sup> cells and their migration to CXCL9. (e) WT (black columns), *Gba1*<sup>9V/-</sup> (maroon columns) and the values shown in the bar diagram are the mean  $\pm$  SD. and group comparison was performed with ANOVA. Three independent experiments were conducted (\*\*\*\*  $p < 0.0001$ ).

### 3.5. Pharmaceutical Targeting of CXCR3 Causes the Reduction of CXCL9 Mediated In Vivo T Cells Chemotaxis in *Gba1*<sup>9V/-</sup> Mice

To confirm if in vivo administration of mouse anti-CXCR3 antibodies decrease the CXCL9-mediated chemotaxis of T cell subsets in GD, WT and *Gba1*<sup>9V/-</sup> mice were treated with CXCL9 and its vehicle (PBS) in the presence and absence of mouse anti-CXCR3 antibodies. The peritoneal cells were analysed for total cell infiltrates as well as the CD3<sup>+</sup>CD4<sup>+</sup> T cells and CD3<sup>+</sup>CD8<sup>+</sup> T cells (see Methods). Compared to vehicle (PBS) or mouse anti-CXCR3 antibodies, administered CXCL9 to WT mice showed increased peritoneal cell recruitment (Supplementary Figure S4a–c,e;  $p < 0.01$ ). Compared to administered CXCL9, mouse anti-CXCR3 antibodies given prior to CXCL9 injection abrogated the CXCL9 mediated increased recruitment of peritoneal cells in WT mice (Supplementary Figure S4c–e;  $p < 0.01$ ). As compared to vehicle or mouse anti-CXCR3 antibodies administration, CXCL9 injected *Gba1*<sup>9V/-</sup> mice showed more pronounced peritoneal cell infiltrates (Supplementary Figure S4f–h and e;  $p < 0.0001$ ). Compared to administered CXCL9, mouse anti-CXCR3 antibodies given prior to CXCL9 injection caused marked reductions in the increased recruitment of peritoneal cells in *Gba1*<sup>9V/-</sup> mice (Supplementary Figure S4e,h,i;  $p < 0.0001$ ). These findings were also obtained for CD4<sup>+</sup> T cells (Figure 6e–i;  $p < 0.0001$ ,  $p < 0.001$ ). In

WT mice, the CD4<sup>+</sup> T cell differences were not significant when compared with vehicle, mouse anti-CXCR3 antibodies, CXCL9 and mouse anti-CXCR3 antibodies administered prior to CXCL9 (Figure 6a–e; ns).

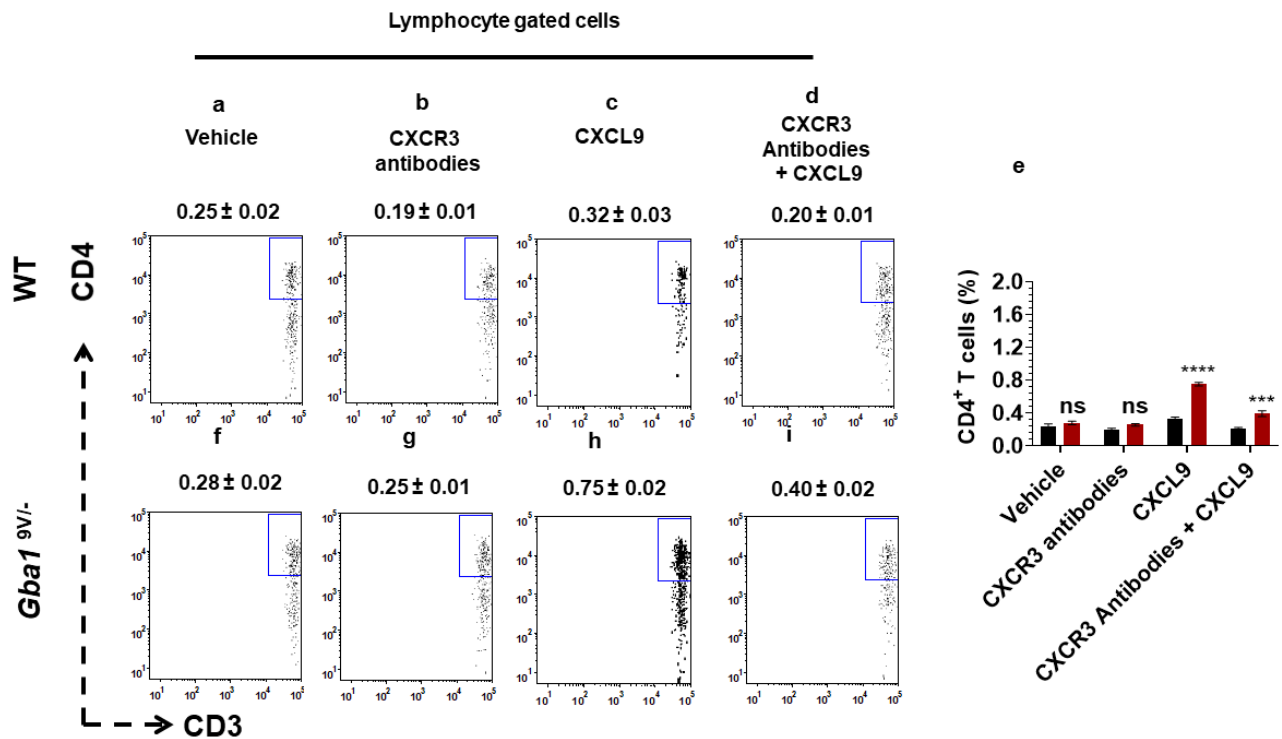


**Figure 6.** In vivo blocking of CXCR3 alters the CXCL9-mediated CD4<sup>+</sup> T cells chemotaxis in *Gba1*<sup>9V/-</sup> mice. WT and *Gba1*<sup>9V/-</sup> mice were injected with intraperitoneal administration of CXCL9 and its vehicle as described in the method. In additional experiments, these mice were injected with intravenous injection of mouse anti-CXCR3 antibodies prior to intraperitoneal injection of CXCL9 or vehicle and the peritoneal cells were collected and analyzed by FACS. The dot plots and the corresponding bar diagrams represent the percentage of migrated CD3<sup>+</sup>CD4<sup>+</sup> T cells in WT (a–e) and *Gba1*<sup>9V/-</sup> mice (e–i). WT (black columns), *Gba1*<sup>9V/-</sup> (maroon columns) and the values shown are the mean ± SD. and group comparison were performed with ANOVA. Three independent experiments were conducted (ns, not significant; \*\*\*,  $p < 0.001$ , \*\*\*\*,  $p < 0.0001$ ).

As compared to PBS or mouse anti-CXCR3 antibodies treated mice, CXCL9 injected *Gba1*<sup>9V/-</sup> mice showed elevated recruitment of peritoneal CD8<sup>+</sup> T cells (Figure 7e–h;  $p < 0.0001$ ), In comparison, mouse anti-CXCR3 antibodies administration prior to giving CXCL9 abrogated the increased recruitment of peritoneal CD8<sup>+</sup> T cells in *Gba1*<sup>9V/-</sup> mice (Figure 7e,h,i;  $p < 0.05$ ). The effects of these treatments on WT CD8<sup>+</sup>-cells were not significant (Figure 7a–e; ns).

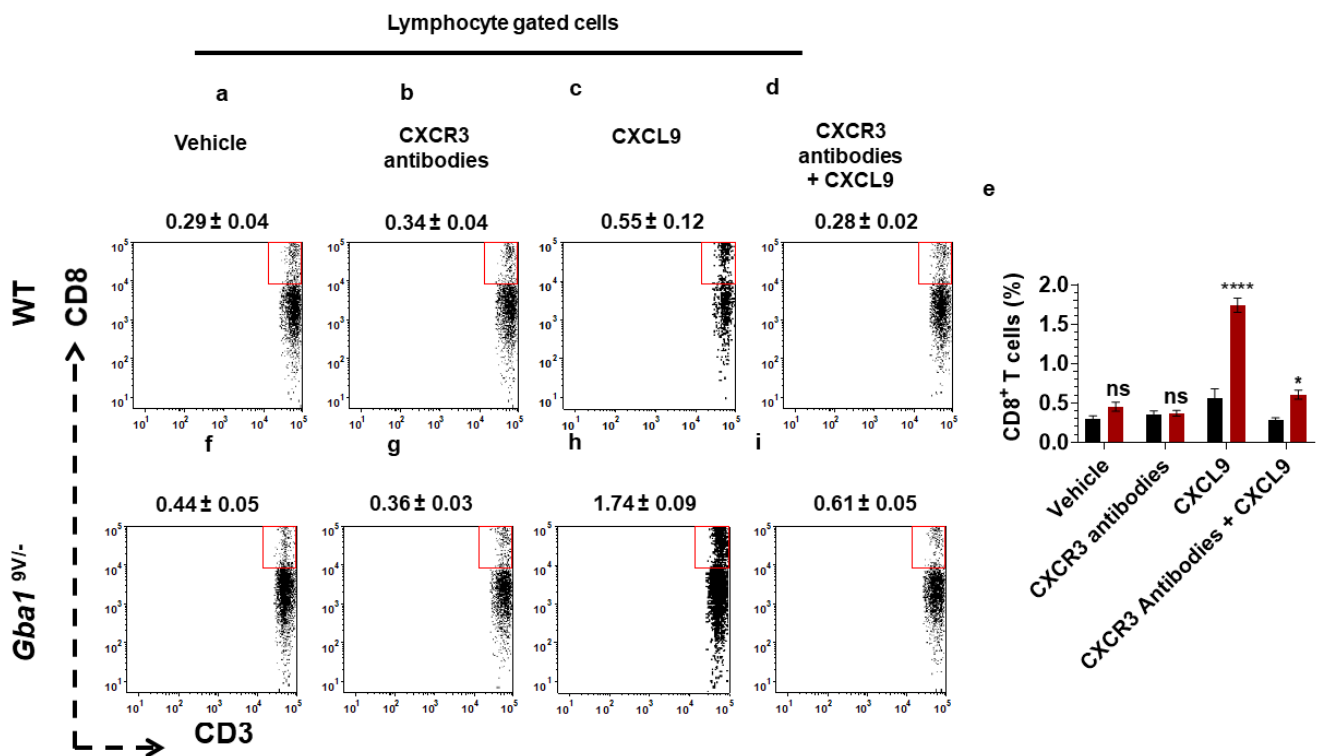


**Figure 7.** In vivo blocking of CXCR3 alters the CXCL9-mediated CD8<sup>+</sup> T cells chemotaxis in *Gba1*<sup>9V/-</sup> mice. WT and *Gba1*<sup>9V/-</sup> mice were injected with intraperitoneal administration of CXCL9 and its vehicle as described in the method. In additional experiments, these mice were injected with intravenous injection of mouse anti-CXCR3 antibodies prior to intraperitoneal injection of CXCL9 or vehicle and the peritoneal cells were collected and analyzed by FACS. The dot plots and the corresponding bar diagrams represent the percentage of migrated CD3<sup>+</sup>CD8<sup>+</sup> T cells in WT (a–e) and *Gba1*<sup>9V/-</sup> mice (e–i). WT (black columns), *Gba1*<sup>9V/-</sup> (maroon columns), and the values shown are the mean  $\pm$  SD. and group comparison were performed with ANOVA. Three independent experiments were conducted (ns, not significant; \*  $p < 0.05$ ; \*\*\*\*  $p < 0.0001$ ).

#### 4. Discussion

Here, M $\phi$ s and DCs have been recognized as the sources of local increases of CXCL9 in *Gba1*<sup>9V/-</sup> mice. Furthermore, CD4<sup>+</sup> T cells and the CD8<sup>+</sup> T cells from *Gba1*<sup>9V/-</sup> mice had increased amounts of CXCR3. Although not explicitly tested, these findings implicate mutant *Gba1* and the resultant excess tissue accumulation of GC in increasing the production/expression of CXCL9 in GD. Such increased CXCL9 directed the chemotaxis of CXCR3 expressing T cell subsets in the *Gba1*<sup>9V/-</sup> mouse model of GD. This is supported by the lung-derived *Gba1*<sup>9V/-</sup> M $\phi$ s and DCs having increased amounts of CXCL9 and the T cell subsets with increased amounts of CXCR3.

In addition, these findings highlight the importance of the CXCL9-CXCR3 axis in the induction of ex vivo and in vivo chemotaxis of CD4<sup>+</sup> and CD8<sup>+</sup> T cells in the *Gba1*<sup>9V/-</sup> mouse.

CXCL9 chemokines attracts CXCR3<sup>+</sup>CD4<sup>+</sup> and CD8<sup>+</sup> effector T cells to sites of inflammation and direct their polarization into highly potent effector T cells that lead to the tissue enlargement in several diseases [64,67,72–84]. Elevated levels of such T cell subsets and their interaction with antigen presenting cells (e.g., DCs and/or M $\phi$ s) are a and, potentially, the major effector contributing to massive increases of pro-inflammatory cytokines and tissue destruction in GD [5,6,15,16,85]. However, the cellular mechanism(s) underlying increased infiltration of T cell subsets in GD are not clearly understood. As compared to CXCL10 and CXCL11, massive increases of CXCL9 in *Gba1*<sup>9V/-</sup> [10] provided the impetus for exploring the role of CXCL9-induced T cell trafficking in GD.

In certain tissues, e.g., lung, intestine, and tumor, cause downregulation of chemokine receptor expression once the infiltrating cells reside in the tissues and are exposed to

high concentrations of ligands and/or interact with abnormal local production of pro-inflammatory cytokines [86–89]. To avoid this limitation, the current study used spleen derived T cells for testing CXCL9-mediated ex-vivo chemotaxis in the *Gba1*<sup>9V/-</sup> mouse. This study identified a direct role of the CXCL9-CXCR3 axis in aiming the excess tissue recruitment of T cells in the *Gba1*<sup>9V/-</sup> mouse. CXCR3 is an attractive therapeutic target for treating T cell-mediated inflammatory diseases [83,84,90–96]. CXCL9-mediated ex vivo and in vivo chemotaxis of T cell subsets (i.e., CD4<sup>+</sup> T and CD8<sup>+</sup> T cells) in the presence or absence of mouse anti-CXCR3 antibodies showed that targeting CXCR3 caused marked reduction in CXCL9-mediated enhanced tissue recruitment of T cell subsets in GD.

The exact mechanism(s) by which immune phagocytes, (e.g., Mφs and DCs) and/or T cells lead to increased levels of CXCL9/CXCR3 in *Gba1*<sup>9V/-</sup> mice remain to be fully elucidated. IFNγ and its downstream signaling is needed for driving CXCL9-CXCR3-mediated tissue inflammation in several diseases [64–70].

Excess tissue amounts of GC, IFNγ, and their downstream effects have been reported in mouse models and human patients with GD [5,6,13,15–17,41–45,47,71]. Additionally, genetic deficiency of C5aR1 resulted in decreased tissue levels of GC, IFNγ, CXCL9–11, and reductions in tissue recruitment of T cell subsets in mouse models of GD [16]. These findings implicate a mechanistic link between GC/C5a-C5aR1-IFNγ pathways for activation of CXCL9/CXCR3 in GD, which require further mechanistic elucidation.

The clinical features of human GD that happens due to *GBA1* defect includes anemia, thrombocytopenia, hypergammaglobulinemia, splenomegaly, hepatomegaly, bone and brain defects) [1,9–12,14]. *Gba1*<sup>9V/-</sup> mouse model of GD recapitulated many of these signs including, tissue accumulation of Gaucher cells and GC in lung, liver, and spleen as well as infiltration of T cells [4,5,13,15–22]. However, there is still some limitations of the study as the *Gba1*<sup>9V/-</sup> mouse model of GD does not recapitulate exactly the human disease and other indicated disease complications.

Mice express a single isoform of CXCR3 that exclusively binds to CXCL9, CXCL10, and CXCL11. CXCR3a, b and alt isoforms exist in humans [97]. Human CXCR3a is equivalent to mouse CXCR3 and binds CXCL9, CXCL10, and CXCL11. Human CXCR3b binds to CXCL9, CXCL10, CXCL11 as well as an additional ligand CXCL4. Human CXCR3alt binds specifically to CXCL11 [97]. The translational potential of this research could be challenging as in contrast to murine CXCL9 and CXCL11, human CXCL9–11 are inactivated rapidly in the presence of physiological concentrations of dipeptidyl peptidase IV/CD26 [98–100]. Despite of these complexities, the current study invites investigation into the different isoforms of CXCR3 and their ligands, i.e., CXCL9–11, as well as their up and/or downstream signaling that enhance T cell trafficking in GD. These findings open new areas of research that may identify CXCR3 and several of their ligands as interesting drug targets for modulation of immune cell function that fuel tissue inflammation in GD and other lysosomal storage sicknesses.

**Supplementary Materials:** The following are available online at <https://www.mdpi.com/article/10.3390/ijms222312712/s1>.

**Author Contributions:** Conceptualization, M.K.P.; methodology, M.K.P., A.F.M., R.R., M.A.M., S.L.H., T.C.N. and D.N.A.M.; formal analysis, M.K.P. and G.A.G.; investigation, M.K.P.; resources, M.K.P. and G.A.G.; data curation, M.K.P. and G.A.G.; writing—original draft preparation, M.K.P. and G.A.G.; writing—review and editing, M.K.P. and G.A.G.; visualization, M.K.P., J.K. and G.A.G.; supervision, M.K.P.; project administration, M.K.P.; funding acquisition, M.K.P. All authors have read and agreed to the published version of the manuscript.

**Funding:** This research received no external funding.

**Institutional Review Board Statement:** Not applicable.

**Informed Consent Statement:** Not applicable.

**Data Availability Statement:** Not applicable.

**Acknowledgments:** This work was supported by Division of Human Genetics, Cincinnati Children's Hospital Medical Center (Cincinnati, OH, USA) to MKP. We thank Cincinnati Children's Innovation Venture Team, Research Flow Cytometry, Pathology, and Animal Cores for their support. We would like to acknowledge Charles D Loftice for office and Laboratory support.

**Conflicts of Interest:** The authors declare that the research was conducted in the absence of any commercial or financial relationships that could be construed as a potential conflict of interest.

## References

1. Motta, I.; Consonni, D.; Stroppiano, M.; Benedetto, C.; Cassinerio, E.; Tappino, B.; Ranalli, P.; Borin, L.; Facchini, L.; Splenomegaly Gaucher Group; et al. Predicting the probability of Gaucher disease in subjects with splenomegaly and thrombocytopenia. *Sci. Rep.* **2021**, *11*, 2594. [[CrossRef](#)]
2. Stirnemann, J.; Belmatoug, N.; Camou, F.; Serratrice, C.; Froissart, R.; Caillaud, C.; Levade, T.; Astudillo, L.; Serratrice, J.; Brassier, A.; et al. A Review of Gaucher Disease Pathophysiology, Clinical Presentation and Treatments. *Int. J. Mol. Sci.* **2017**, *18*, 441. [[CrossRef](#)] [[PubMed](#)]
3. Grabowski, G.A.; Petsko, G.A.; Kolodny, E.H. Gaucher Disease. In *The Online Metabolic and Molecular Bases of Inherited Disease*, 146th ed.; McGraw Hill: New York, NY, USA, 2010; pp. 1–13.
4. Xu, Y.H.; Quinn, B.; Witte, D.; Grabowski, G.A. Viable mouse models of acid beta-glucosidase deficiency: The defect in Gaucher disease. *Am. J. Pathol.* **2003**, *163*, 2093–2101. [[CrossRef](#)]
5. Pandey, M.K.; Grabowski, G.A. Cytology of Gaucher disease. In *Advances in Gaucher Disease: Basic and Clinical Perspectives*; Future Medicine Ltd.: London, UK, 2013; pp. 78–93.
6. Pandey, M.K.; Grabowski, G.A. Immunological Cells and Functions in Gaucher Disease. *Crit. Rev. Oncog.* **2013**, *18*, 197–220. [[CrossRef](#)] [[PubMed](#)]
7. van Eijk, M.; Aerts, J.M.F.G. The Unique Phenotype of Lipid-Laden Macrophages. *Int. J. Mol. Sci.* **2021**, *22*, 4039. [[CrossRef](#)]
8. Serfecz, J.C.; Saadin, A.; Santiago, C.P.; Zhang, Y.; Bentzen, S.M.; Vogel, S.N.; Feldman, R.A. C5a Activates a Pro-Inflammatory Gene Expression Profile in Human Gaucher iPSC-Derived Macrophages. *Int. J. Mol. Sci.* **2021**, *22*, 9912. [[CrossRef](#)] [[PubMed](#)]
9. Andrade-Campos, M.; Alfonso, P.; Irun, P.; Armstrong, J.; Calvo, C.; Dalmau, J.; Domingo, M.-R.; Barbera, J.-L.; Cano, H.; Fernandez-Galán, M.-A.; et al. Diagnosis features of pediatric Gaucher disease patients in the era of enzymatic therapy, a national-base study from the Spanish Registry of Gaucher Disease. *Orphanet J. Rare Dis.* **2017**, *12*, 84. [[CrossRef](#)]
10. Mehta, A.; Kuter, D.J.; Salek, S.S.; Belmatoug, N.; Bembi, B.; Bright, J.; Dahl, S.V.; Deodato, F.; Di Rocco, M.; Göker-Alpan, O.; et al. Presenting signs and patient co-variables in Gaucher disease: Outcome of the Gaucher Earlier Diagnosis Consensus (GED-C) Delphi initiative. *Intern. Med. J.* **2018**, *49*, 578–591. [[CrossRef](#)]
11. Charrow, J.; Andersson, H.C.; Kaplan, P.; Kolodny, E.H.; Mistry, P.; Pastores, G.; Rosenbloom, B.E.; Scott, C.R.; Wappner, R.S.; Weinreb, N.J.; et al. The Gaucher Registry. *Arch. Intern. Med.* **2000**, *160*, 2835–2843. [[CrossRef](#)]
12. Magnusen, A.F.; Hatton, S.L.; Rani, R.; Pandey, M.K. Genetic Defects and Pro-inflammatory Cytokines in Parkinson's Disease. *Front. Neurol.* **2021**, *12*, 881. [[CrossRef](#)]
13. Xu, Y.-H.; Jia, L.; Quinn, B.; Zamzow, M.; Stringer, K.; Aronow, B.; Sun, Y.; Zhang, W.; Setchell, K.D.; A Grabowski, G. Global gene expression profile progression in Gaucher disease mouse models. *BMC Genom.* **2011**, *12*, 20. [[CrossRef](#)] [[PubMed](#)]
14. Grabowski, G.A.; Antommaria, A.H.; Kolodny, E.H.; Mistry, P.K. Gaucher disease: Basic and translational science needs for more complete therapy and management. *Mol. Genet. Metab.* **2020**, *132*, 59–75. [[CrossRef](#)]
15. Pandey, M.K.; Rani, R.; Zhang, W.; Setchell, K.; Grabowski, G.A. Immunological cell type characterization and Th1–Th17 cytokine production in a mouse model of Gaucher disease. *Mol. Genet. Metab.* **2012**, *106*, 310–322. [[CrossRef](#)] [[PubMed](#)]
16. Pandey, M.K.; Burrow, T.A.; Rani, R.; Martin, L.J.; Witte, D.; Setchell, K.D.; McKay, M.A.; Magnusen, A.F.; Zhang, K.D.S.W.; Liou, B.; et al. Complement drives glucosylceramide accumulation and tissue inflammation in Gaucher disease. *Nature* **2017**, *543*, 108–112. [[CrossRef](#)]
17. Pandey, M.K.; Jabre, N.A.; Xu, Y.-H.; Zhang, W.; Setchell, K.D.; Grabowski, G.A. Gaucher disease: Chemotactic factors and immunological cell invasion in a mouse model. *Mol. Genet. Metab.* **2014**, *111*, 163–171. [[CrossRef](#)] [[PubMed](#)]
18. Dasgupta, N.; Xu, Y.-H.; Oh, S.; Sun, Y.; Jia, L.; Keddache, M.; A Grabowski, G. Gaucher Disease: Transcriptome Analyses Using Microarray or mRNA Sequencing in a Gba1 Mutant Mouse Model Treated with Velaglucerase alfa or Imiglucerase. *PLoS ONE* **2013**, *8*, e74912. [[CrossRef](#)]
19. Dasgupta, N.; Xu, Y.-H.; Li, R.; Peng, Y.; Pandey, M.K.; Tinch, S.L.; Liou, B.; Inskeep, V.; Zhang, W.; Setchell, K.D.; et al. Neuronopathic Gaucher disease: Dysregulated mRNAs and miRNAs in brain pathogenesis and effects of pharmacologic chaperone treatment in a mouse model. *Hum. Mol. Genet.* **2015**, *24*, 7031–7048. [[CrossRef](#)]
20. Barnes, S.; Xu, Y.-H.; Zhang, W.; Liou, B.; Setchell, K.D.R.; Bao, L.; Grabowski, G.A.; Sun, Y. Ubiquitous Transgene Expression of the Glucosylceramide-Synthesizing Enzyme Accelerates Glucosylceramide Accumulation and Storage Cells in a Gaucher Disease Mouse Model. *PLoS ONE* **2014**, *9*, e116023. [[CrossRef](#)]
21. Sun, Y.; Zhang, W.; Xu, Y.-H.; Quinn, B.; Dasgupta, N.; Liou, B.; Setchell, K.D.R.; Grabowski, G.A. Substrate Compositional Variation with Tissue/Region and Gba1 Mutations in Mouse Models—Implications for Gaucher Disease. *PLoS ONE* **2013**, *8*, e57560.

22. Liou, B.; Zhang, W.; Fannin, V.; Quinn, B.; Ran, H.; Xu, K.; Setchell, K.D.R.; Witte, D.; Grabowski, G.A.; Sun, Y. Combination of acid  $\beta$ -glucosidase mutation and Saposin C deficiency in mice reveals Gba1 mutation dependent and tissue-specific disease phenotype. *Sci. Rep.* **2019**, *9*, 5571. [[CrossRef](#)]
23. D'Amico, G.; Bonamino, M.; Dander, E.; Marin, V.; Basso, G.; Balduzzi, A.; Biagi, E.; Biondi, A. T cells stimulated by CD40L positive leukemic blasts-pulsed dendritic cells meet optimal functional requirements for adoptive T-cell therapy. *Leukemia* **2006**, *20*, 2015–2024. [[CrossRef](#)] [[PubMed](#)]
24. Hu, W.; Wang, Z.-M.; Feng, Y.; Schizas, M.; Hoyos, B.E.; van der Veeken, J.; Verter, J.G.; Bou-Puerto, R.; Rudensky, A.Y. Regulatory T cells function in established systemic inflammation and reverse fatal autoimmunity. *Nat. Immunol.* **2021**, *22*, 1163–1174. [[CrossRef](#)] [[PubMed](#)]
25. Kim, S.-H.; Cho, E.; Kim, Y.I.; Han, C.; Choi, B.K.; Kwon, B.S. Adoptive immunotherapy with transient anti-CD4 treatment enhances anti-tumor response by increasing IL-18R $\alpha$ hi CD8<sup>+</sup> T cells. *Nat. Commun.* **2021**, *12*, 5314. [[CrossRef](#)]
26. Sakaguchi, S. Naturally arising Foxp3-expressing CD25<sup>+</sup>CD4<sup>+</sup> regulatory T cells in immunological tolerance to self and non-self. *Nat. Immunol.* **2005**, *6*, 345–352. [[CrossRef](#)] [[PubMed](#)]
27. Farber, D.L. Form and function for T cells in health and disease. *Nat. Rev. Immunol.* **2019**, *20*, 83–84. [[CrossRef](#)] [[PubMed](#)]
28. Sun, J.C.; Williams, M.A.; Bevan, M.J. CD4<sup>+</sup> T cells are required for the maintenance, not programming, of memory CD8<sup>+</sup> T cells after acute infection. *Nat. Immunol.* **2004**, *5*, 927–933. [[CrossRef](#)] [[PubMed](#)]
29. Shenoy, A.T.; De Ana, C.L.; Arafa, E.I.; Salwig, I.; Barker, K.A.; Korkmaz, F.T.; Ramanujan, A.; Etesami, N.S.; Soucy, A.M.; Martin, I.M.C.; et al. Antigen presentation by lung epithelial cells directs CD4<sup>+</sup> TRM cell function and regulates barrier immunity. *Nat. Commun.* **2021**, *12*, 5834. [[CrossRef](#)] [[PubMed](#)]
30. Bestebroer, J.; Aerts, P.C.; Rooijackers, S.H.M.; Pandey, M.K.; Köhl, J.; Van Strijp, J.A.G.; De Haas, C.J.C. Functional basis for complement evasion by staphylococcal superantigen-like 7. *Cell. Microbiol.* **2010**, *12*, 1506–1516. [[CrossRef](#)] [[PubMed](#)]
31. Mosmann, T.R.; Coffman, R.L. TH1 and TH2 cells: Different patterns of lymphokine secretion lead to different functional properties. *Annu. Rev. Immunol.* **1989**, *7*, 145–173. [[CrossRef](#)]
32. Korn, T.; Bettelli, E.; Oukka, M.; Kuchroo, V.K. IL-17 and Th17 Cells. *Annu. Rev. Immunol.* **2009**, *27*, 485–517. [[CrossRef](#)] [[PubMed](#)]
33. Kiner, E.; Willie, E.; Vijaykumar, B.; Chowdhary, K.; Schmutz, H.; Chandler, J.; Schnell, A.; Thakore, P.I.; LeGros, G.; Mostafavi, S.; et al. Gut CD4<sup>+</sup> T cell phenotypes are a continuum molded by microbes, not by TH archetypes. *Nat. Immunol.* **2021**, *22*, 216–228. [[CrossRef](#)]
34. Becattini, S.; Latorre, D.; Mele, F.; Foglierini, M.; De Gregorio, C.; Cassotta, A.; Fernandez, B.; Kelderman, S.; Schumacher, T.; Corti, D.; et al. T cell immunity. Functional heterogeneity of human memory CD4<sup>+</sup> T cell clones primed by pathogens or vaccines. *Science* **2015**, *347*, 400–406. [[CrossRef](#)] [[PubMed](#)]
35. Weaver, D.J., Jr.; Reis, E.S.; Pandey, M.K.; Köhl, G.; Harris, N.; Gerard, C.; Koehl, J. C5a receptor-deficient dendritic cells promote induction of Treg and Th17 cells. *Eur. J. Immunol.* **2010**, *40*, 710–721. [[CrossRef](#)] [[PubMed](#)]
36. Zhang, X.; Schmutz, I.; Laumonier, Y.; Pandey, M.K.; Clark, J.R.; König, P.; Gerard, N.P.; Gerard, C.; Wills-Karp, M.; Köhl, J. A Critical Role for C5L2 in the Pathogenesis of Experimental Allergic Asthma. *J. Immunol.* **2010**, *185*, 6741–6752. [[CrossRef](#)] [[PubMed](#)]
37. Bevan, M.J. Helping the CD8<sup>+</sup> T-cell response. *Nat. Rev. Immunol.* **2004**, *4*, 595–602. [[CrossRef](#)]
38. Gangaev, A.; Ketelaars, S.L.C.; Isaeva, O.I.; Patiwaal, S.; Dopler, A.; Hoefakker, K.; De Biasi, S.; Gibellini, L.; Mussini, C.; Guaraldi, G.; et al. Identification and characterization of a SARS-CoV-2 specific CD8<sup>+</sup> T cell response with immunodominant features. *Nat. Commun.* **2021**, *12*, 2593. [[CrossRef](#)] [[PubMed](#)]
39. Philip, M.; Schietinger, A. CD8<sup>+</sup> T cell differentiation and dysfunction in cancer. *Nat. Rev. Immunol.* **2021**, 1–15. [[CrossRef](#)]
40. Buang, N.; Tapeng, L.; Gray, V.; Sardini, A.; Whilding, C.; Lightstone, L.; Cairns, T.D.; Pickering, M.C.; Behmoaras, J.; Ling, G.S.; et al. Type I interferons affect the metabolic fitness of CD8<sup>+</sup> T cells from patients with systemic lupus erythematosus. *Nat. Commun.* **2021**, *12*, 1980. [[CrossRef](#)] [[PubMed](#)]
41. Nair, S.; Boddupalli, C.S.; Verma, R.; Liu, J.; Yang, R.; Pastores, G.M.; Mistry, P.K.; Dhodapkar, M.V. Type II NKT-TFH cells against Gaucher lipids regulate B-cell immunity and inflammation. *Blood* **2015**, *125*, 1256–1271. [[CrossRef](#)]
42. Lingala, R.P.; Ioanou, C.; Plassmeyer, M.; Ryherd, M.; Kozhaya, L.; Austin, L.; Abidoglu, C.; Unutmaz, D.; Alpan, O.; Göker-Alpan, O. Time of Initiating Enzyme Replacement Therapy Affects Immune Abnormalities and Disease Severity in Patients with Gaucher Disease. *PLoS ONE* **2016**, *11*, e0168135. [[CrossRef](#)]
43. Sotiropoulos, C.; Theodorou, G.; Repa, C.; Marinakis, T.; Verigou, E.; Solomou, E.; Karakantza, M.; Symeonidis, A.; Zschocke, J.; Baumgartner, M.; et al. Severe impairment of regulatory T-cells and Th1-lymphocyte polarization in patients with Gaucher disease. *JIMD Rep.* **2015**, *18*, 107–115. [[PubMed](#)]
44. Zahran, A.M.; Eltayeb, A.A.; Elsayh, K.I.; Saad, K.; Ahmad, F.-A.; Ibrahim, A.I.M. Activated and Memory T Lymphocytes in Children with Gaucher Disease. *Arch. Immunol. Ther. Exp.* **2016**, *65*, 263–269. [[CrossRef](#)]
45. Zahran, A.M.; Youssef, M.A.M.; Shafik, E.A.; Zahran, Z.A.M.; El-Badawy, O.; Elgheet, A.M.A.; Elsayh, K.I. Downregulation of B regulatory cells and upregulation of T helper 1 cells in children with Gaucher disease undergoing enzyme replacement therapy. *Immunol. Res.* **2020**, *68*, 73–80. [[CrossRef](#)]
46. Zahran, A.M.; Saad, K.; Abo-Elam, M.G.; Elouseily, E.M.; Gad, E.F.; Abo Elgheet, A.M.; Mahmmoud, R.R.; Youssef, M.A.M.; Abdelmeguid, M.M.; Hawary, B.; et al. Down-regulation of Regulatory T-cells in Children With Gaucher Disease Under Enzyme Replacement Therapy. *Clin. Appl. Thromb. Hemost.* **2019**, *25*, 1076029619889685. [[CrossRef](#)] [[PubMed](#)]

47. Liu, J.; Halene, S.; Yang, M.; Iqbal, J.; Yang, R.; Mehal, W.Z.; Chuang, W.-L.; Jain, D.; Yuen, T.; Sun, L.; et al. Gaucher disease gene GBA functions in immune regulation. *Proc. Natl. Acad. Sci. USA* **2012**, *109*, 10018–10023. [[CrossRef](#)] [[PubMed](#)]
48. Yamamoto, J.; Adachi, Y.S.; Onoue, Y.; Okabe, Y.; Itazawa, T.; Toyoda, M.; Seki, T.; Morohashi, M.; Matsushima, K.; Miyawaki, T. Differential expression of the chemokine receptors by the Th1- and Th2-type effector populations within circulating CD4<sup>+</sup> T cells. *J. Leukoc. Biol.* **2000**, *68*, 568–574. [[PubMed](#)]
49. Loetscher, M.; Gerber, B.; Jones, S.A.; Piali, L.; Clark-Lewis, I.; Baggiolini, M.; Moser, B. Chemokine receptor specific for IP10 and mig: Structure, function, and expression in activated T-lymphocytes. *J. Exp. Med.* **1996**, *184*, 963–969. [[CrossRef](#)] [[PubMed](#)]
50. Farber, J.M. Mig and IP-10: CXC chemokines that target lymphocytes. *J. Leukoc. Biol.* **1997**, *61*, 246–257. [[CrossRef](#)] [[PubMed](#)]
51. Cole, K.E.; Strick, C.A.; Paradis, T.J.; Ogborne, K.T.; Loetscher, M.; Gladue, R.P.; Lin, W.; Boyd, J.G.; Moser, B.; Wood, D.E.; et al. Interferon-inducible T Cell Alpha Chemoattractant (I-TAC): A Novel Non-ELR CXC Chemokine with Potent Activity on Activated T Cells through Selective High Affinity Binding to CXCR3. *J. Exp. Med.* **1998**, *187*, 2009–2021. [[CrossRef](#)]
52. Loetscher, M.; Loetscher, P.; Brass, N.; Meese, E.; Moser, B. Lymphocyte-specific chemokine receptor CXCR3: Regulation, chemokine binding and gene localization. *Eur. J. Immunol.* **1998**, *28*, 3696–3705. [[CrossRef](#)]
53. Luster, A.D. Chemokines-Chemotactic cytokines that mediate inflammation. *N. Engl. J. Med.* **1998**, *338*, 436–445. [[CrossRef](#)]
54. Soto, H.; Wang, W.; Strieter, R.M.; Copeland, N.G.; Gilbert, D.J.; Jenkins, N.A.; Hedrick, J.; Zlotnik, A. The CC chemokine 6Ckine binds the CXC chemokine receptor CXCR3. *Proc. Natl. Acad. Sci. USA* **1998**, *95*, 8205–8210. [[CrossRef](#)] [[PubMed](#)]
55. Cella, M.; Jarrossay, D.; Facchetti, F.; Alebardi, O.; Nakajima, H.; Lanzavecchia, A.; Colonna, M. Plasmacytoid monocytes migrate to inflamed lymph nodes and produce large amounts of type I interferon. *Nat. Med.* **1999**, *5*, 919–923. [[CrossRef](#)]
56. Tensen, C.; Flier, J.; van der Raaij-Helmer, E.M.; Sampat-Sardjoepersad, S.; van der Schors, R.C.; Leurs, R.; Scheper, R.J.; Boorsma, D.M.; Willemze, R. Human IP-9: A Keratinocyte-Derived High Affinity CXC-Chemokine Ligand for the IP-10/Mig Receptor (CXCR3)1. *J. Investig. Dermatol.* **1999**, *112*, 716–722. [[CrossRef](#)] [[PubMed](#)]
57. García-López, M.; Sánchez-Madrid, F.; Frade, J.M.R.; Mellado, M.; Acevedo, A.; Garcia, M.A.; Albar, J.P.; Martínez-A, C.; Marazuela, M. CXCR3 Chemokine Receptor Distribution in Normal and Inflamed Tissues: Expression on Activated Lymphocytes, Endothelial Cells, and Dendritic Cells. *Lab. Invest.* **2001**, *81*, 409–418. [[CrossRef](#)]
58. Sallusto, F.; Kremmer, E.; Palermo, B.; Hoy, A.; Ponath, P.; Qin, S.; Forster, R.; Lipp, M.; Lanzavecchia, A. Switch in chemokine receptor expression upon TCR stimulation reveals novel homing potential for recently activated T cells. *Eur. J. Immunol.* **1999**, *29*, 2037–2045. [[CrossRef](#)]
59. Sallusto, F.; Lanzavecchia, A.; Mackay, C.R. Chemokines and chemokine receptors in T-cell priming and Th1/Th2-mediated responses. *Immunol. Today* **1998**, *19*, 568–574. [[CrossRef](#)]
60. Fukuda, Y.; Asaoka, T.; Eguchi, H.; Yokota, Y.; Kubo, M.; Kinoshita, M.; Urakawa, S.; Iwagami, Y.; Tomimaru, Y.; Akita, H.; et al. Endogenous CXCL9 affects prognosis by regulating tumor-infiltrating natural killer cells in intrahepatic cholangiocarcinoma. *Cancer Sci.* **2019**, *111*, 323–333. [[CrossRef](#)] [[PubMed](#)]
61. Lacotte, S.; Brun, S.; Muller, S.; Dumortier, H. CXCR3, inflammation, and autoimmune diseases. *Ann. N. Y. Acad. Sci.* **2009**, *1173*, 310–317. [[CrossRef](#)]
62. Enghard, P.; Humrich, J.Y.; Rudolph, B.; Rosenberger, S.; Biesen, R.; Kuhn, A.; Manz, R.; Hiepe, F.; Radbruch, A.; Burmester, G.-R.; et al. CXCR3<sup>+</sup>CD4<sup>+</sup> T cells are enriched in inflamed kidneys and urine and provide a new biomarker for acute nephritis flares in systemic lupus erythematosus patients. *Arthritis Rheum.* **2008**, *60*, 199–206. [[CrossRef](#)]
63. Watanabe, T.; Suzuki, J.; Mitsuo, A.; Nakano, S.; Tamayama, Y.; Katagiri, A.; Amano, H.; Morimoto, S.; Tokano, Y.; Takasaki, Y. Striking alteration of some populations of T/B cells in systemic lupus erythematosus: Relationship to expression of CD62L or some chemokine receptors. *Lupus* **2008**, *17*, 26–33. [[CrossRef](#)]
64. Groom, J.R.; Luster, A.D. CXCR3 in T cell function. *Exp. Cell Res.* **2011**, *317*, 620–631. [[CrossRef](#)] [[PubMed](#)]
65. Liu, L.; Callahan, M.K.; Huang, D.; Ransohoff, R.M. Chemokine receptor CXCR3: An unexpected enigma. *Curr. Top. Dev. Biol.* **2005**, *68*, 149–181. [[PubMed](#)]
66. Rotondi, M.; Chiovato, L.; Romagnani, S.; Serio, M.; Romagnani, P. Role of Chemokines in Endocrine Autoimmune Diseases. *Endocr. Rev.* **2007**, *28*, 492–520. [[CrossRef](#)]
67. Menke, J.; Zeller, G.C.; Kikawada, E.; Means, T.K.; Huang, X.R.; Lan, H.Y.; Lu, B.; Farber, J.; Luster, A.D.; Kelley, V.R. CXCL9, but not CXCL10, Promotes CXCR3-Dependent Immune-Mediated Kidney Disease. *J. Am. Soc. Nephrol.* **2008**, *19*, 1177–1189. [[CrossRef](#)] [[PubMed](#)]
68. Meller, S.; Winterberg, F.; Gilliet, M.; Müller, A.; Lauceviciute, I.; Rieker, J.; Neumann, N.J.; Kubitz, R.; Gombert, M.; Büneemann, E.; et al. Ultraviolet radiation-induced injury, chemokines, and leukocyte recruitment: An amplification cycle triggering cutaneous lupus erythematosus. *Arthritis Rheum.* **2005**, *52*, 1504–1516. [[CrossRef](#)]
69. Farber, J.M. HuMig: A new human member of the chemokine family of cytokines. *Biochem. Biophys. Res. Commun.* **1993**, *192*, 223–230. [[CrossRef](#)] [[PubMed](#)]
70. Nakajima, C.; Mukai, T.; Yamaguchi, N.; Morimoto, Y.; Park, W.R.; Iwasaki, M.; Gao, P.; Ono, S.; Fujiawara, H.; Hamaoka, T. Induction of the chemokine receptor CXCR3 on TCR-stimulated T cells: Dependence on the release from persistent TCR-triggering and requirement for IFN-gamma stimulation. *Eur. J. Immunol.* **2002**, *32*, 1792–1801. [[CrossRef](#)]
71. Jian, J.; Chen, Y.; Liberti, R.; Fu, W.; Hu, W.; Saunders-Pullman, R.; Pastores, G.M.; Chen, Y.; Sun, Y.; Grabowski, G.A.; et al. Chitinase-3-like Protein 1: A Progranulin Downstream Molecule and Potential Biomarker for Gaucher Disease. *EBioMedicine* **2018**, *28*, 251–260. [[CrossRef](#)]

72. Flier, J.; Boorsma, D.M.; van Beek, P.J.; Nieboer, C.; Stoof, T.J.; Willemze, R.; Tensen, C.P. Differential expression of CXCR3 targeting chemokines CXCL10, CXCL9, and CXCL11 in different types of skin inflammation. *J. Pathol.* **2001**, *194*, 398–405. [[CrossRef](#)]
73. Paust, H.-J.; Riedel, J.-H.; Krebs, C.; Turner, J.-E.; Brix, S.R.; Krohn, S.; Velden, J.; Wiech, T.; Kaffke, A.; Peters, A.; et al. CXCR3<sup>+</sup> Regulatory T Cells Control TH1 Responses in Crescentic GN. *J. Am. Soc. Nephrol.* **2015**, *27*, 1933–1942. [[CrossRef](#)]
74. Maurice, N.J.; McElrath, M.J.; Andersen-Nissen, E.; Frahm, N.; Prlic, M. CXCR3 enables recruitment and site-specific bystander activation of memory CD8<sup>+</sup> T cells. *Nat. Commun.* **2019**, *10*, 4987. [[CrossRef](#)] [[PubMed](#)]
75. Qin, S.; Rottman, J.B.; Myers, P.; Kassam, N.; Weinblatt, M.; Loetscher, M.; Koch, A.E.; Moser, B.; Mackay, C. The chemokine receptors CXCR3 and CCR5 mark subsets of T cells associated with certain inflammatory reactions. *J. Clin. Investig.* **1998**, *101*, 746–754. [[CrossRef](#)]
76. Thomas, S.; Banerji, A.; Medoff, B.; Lilly, C.M.; Luster, A.D. Multiple Chemokine Receptors, Including CCR6 and CXCR3, Regulate Antigen-Induced T Cell Homing to the Human Asthmatic Airway. *J. Immunol.* **2007**, *179*, 1901–1912. [[CrossRef](#)]
77. Croudace, J.E.; Inman, C.F.; Abbotts, B.E.; Nagra, S.; Nunnick, J.; Mahendra, P.; Craddock, C.; Malladi, R.; Moss, P.A.H. Chemokine-mediated tissue recruitment of CXCR3<sup>+</sup>CD4<sup>+</sup> T cells plays a major role in the pathogenesis of chronic GVHD. *Blood* **2012**, *120*, 4246–4255. [[CrossRef](#)] [[PubMed](#)]
78. Geiger, B.; Wenzel, J.; Hantschke, M.; Haase, I.; Ständer, S.; Von Stebut, E. Resolving lesions in human cutaneous leishmaniasis predominantly harbour chemokine receptor CXCR3-positive T helper 1/T cytotoxic type 1 cells. *Br. J. Dermatol.* **2010**, *162*, 870–874. [[CrossRef](#)]
79. Zhou, J.; Yu, Q. Disruption of CXCR3 function impedes the development of Sjögren’s syndrome-like xerostomia in non-obese diabetic mice. *Lab. Investig.* **2018**, *98*, 620–628. [[CrossRef](#)] [[PubMed](#)]
80. Mikucki, M.E.; Fisher, D.T.; Matsuzaki, J.; Skitzki, J.J.; Gaulin, N.B.; Muhitch, J.B.; Ku, A.W.; Frelinger, J.G.; Odunsi, K.; Gajewski, T.F.; et al. Non-redundant requirement for CXCR3 signalling during tumoricidal T-cell trafficking across tumour vascular checkpoints. *Nat. Commun.* **2015**, *6*, 7458. [[CrossRef](#)] [[PubMed](#)]
81. Karin, N. CXCR3 Ligands in Cancer and Autoimmunity, Chemoattraction of Effector T Cells, and Beyond. *Front. Immunol.* **2020**, *11*, 976. [[CrossRef](#)]
82. Kunz, M.; Toksoy, A.; Goebeler, M.; Engelhardt, E.; Gillitzer, R. Strong expression of the lymphoattractant C-X-C chemokine Mig is associated with heavy infiltration of T cells in human malignant melanoma. *J. Pathol.* **1999**, *189*, 552–558. [[CrossRef](#)]
83. Frigerio, S.; Junt, T.; Lu, B.; Gerard, C.; Zumsteg, U.; Holländer, G.A.; Piali, L.  $\beta$  cells are responsible for CXCR3-mediated T-cell infiltration in insulinitis. *Nat. Med.* **2002**, *8*, 1414–1420. [[CrossRef](#)]
84. Steinmetz, O.M.; Turner, J.-E.; Paust, H.-J.; Lindner, M.; Peters, A.; Heiss, K.; Velden, J.; Hopfer, H.; Fehr, S.; Krieger, T.; et al. CXCR3 Mediates Renal Th1 and Th17 Immune Response in Murine Lupus Nephritis. *J. Immunol.* **2009**, *183*, 4693–4704. [[CrossRef](#)] [[PubMed](#)]
85. Mistry, P.K.; Liu, J.; Yang, M.; Nottoli, T.; McGrath, J.; Jain, D.; Zhang, K.; Keutzer, J.; Chuang, W.-L.; Mehal, W.Z.; et al. Glucocerebrosidase gene-deficient mouse recapitulates Gaucher disease displaying cellular and molecular dysregulation beyond the macrophage. *Proc. Natl. Acad. Sci. USA* **2010**, *107*, 19473–19478. [[CrossRef](#)]
86. Chakraborty, R.; Rooney, C.; Dotti, G.; Savoldo, B. Changes in Chemokine Receptor Expression of Regulatory T Cells After Ex Vivo Culture. *J. Immunother.* **2012**, *35*, 329–336. [[CrossRef](#)]
87. Wadwa, M.; Klopffleisch, R.; Adamczyk, A.; Frede, A.; Pastille, E.; Mahnke, K.; Hansen, W.; Geffers, R.; Lang, K.; Buer, J.; et al. IL-10 downregulates CXCR3 expression on Th1 cells and interferes with their migration to intestinal inflammatory sites. *Mucosal Immunol.* **2016**, *9*, 1263–1277. [[CrossRef](#)] [[PubMed](#)]
88. Winter, D.; Moser, J.; Kriehuber, E.; Wiesner, C.; Knobler, R.; Trautinger, F.; Bombosi, P.; Stingl, G.; Petzelbauer, P.; Rot, A.; et al. Down-modulation of CXCR3 surface expression and function in CD8<sup>+</sup> T cells from cutaneous T cell lymphoma patients. *J. Immunol.* **2007**, *179*, 4272–4282. [[CrossRef](#)] [[PubMed](#)]
89. Wang, D.; Yu, W.; Lian, J.; Wu, Q.; Liu, S.; Yang, L.; Li, F.; Huang, L.; Chen, X.; Zhang, Z.; et al. Th17 cells inhibit CD8<sup>+</sup> T cell migration by systematically downregulating CXCR3 expression via IL-17A/STAT3 in advanced-stage colorectal cancer patients. *J. Hematol. Oncol.* **2020**, *13*, 68. [[CrossRef](#)]
90. Rashighi, M.; Agarwal, P.; Richmond, J.M.; Harris, T.H.; Dresser, K.; Su, M.-W.; Zhou, Y.; Deng, A.; Hunter, C.A.; Luster, A.D.; et al. CXCL10 Is Critical for the Progression and Maintenance of Depigmentation in a Mouse Model of Vitiligo. *Sci. Transl. Med.* **2014**, *6*, 223ra23. [[CrossRef](#)]
91. Sporici, R.; Issekutz, T.B. CXCR3 blockade inhibits T-cell migration into the CNS during EAE and prevents development of adoptively transferred, but not actively induced, disease. *Eur. J. Immunol.* **2010**, *40*, 2751–2761. [[CrossRef](#)]
92. Dai, Z.; Xing, L.; Cerise, J.; Wang, E.H.C.; Jabbari, A.; De Jong, A.; Petukhova, L.; Christiano, A.M.; Clynes, R. CXCR3 Blockade Inhibits T Cell Migration into the Skin and Prevents Development of Alopecia Areata. *J. Immunol.* **2016**, *197*, 1089–1099. [[CrossRef](#)]
93. Liu, Q.-Z.; Ma, W.-T.; Yang, J.-B.; Zhao, Z.-B.; Yan, K.; Yao, Y.; Li, L.; Miao, Q.; Gershwin, M.E.; Lian, Z.-X. The CXC Chemokine Receptor 3 Inhibits Autoimmune Cholangitis via CD8<sup>+</sup> T Cells but Promotes Colitis via CD4<sup>+</sup> T Cells. *Front. Immunol.* **2018**, *9*, 1090. [[CrossRef](#)]
94. Schroepf, S.; Kappler, R.; Brand, S.; Prell, C.; Lohse, P.; Glas, J.; Hoster, E.; Helmbrecht, J.; Ballauff, A.; Berger, M.; et al. Strong overexpression of CXCR3 axis components in childhood inflammatory bowel disease. *Inflamm. Bowel Dis.* **2010**, *16*, 1882–1890. [[CrossRef](#)] [[PubMed](#)]

95. Jenh, C.-H.; Cox, M.A.; Cui, L.; Reich, E.P.; Sullivan, L.; Chen, S.C.; Kinsley, D.; Qian, S.; Kim, S.H.; Rosenblum, S.; et al. A selective and potent CXCR3 antagonist SCH 546738 attenuates the development of autoimmune diseases and delays graft rejection. *BMC Immunol.* **2012**, *13*, 2. [[CrossRef](#)] [[PubMed](#)]
96. O'Boyle, G.; Fox, C.R.J.; Walden, H.R.; Willet, J.D.P.; Mavin, E.R.; Hine, D.W.; Palmer, J.M.; Barker, C.E.; Lamb, C.; Ali, S.; et al. Chemokine receptor CXCR3 agonist prevents human T-cell migration in a humanized model of arthritic inflammation. *Proc. Natl. Acad. Sci. USA* **2012**, *109*, 4598–4603. [[CrossRef](#)]
97. Korniejewska, A.; McKnight, A.J.; Johnson, Z.; Watson, M.L.; Ward, S.G. Expression and agonist responsiveness of CXCR3 variants in human T lymphocytes. *Immunology* **2011**, *132*, 503–515. [[CrossRef](#)]
98. Mortier, A.; Gouwy, M.; Van Damme, J.; Proost, P.; Struyf, S. CD26/dipeptidylpeptidase IV—Chemokine interactions: Double-edged regulation of inflammation and tumor biology. *J. Leukoc. Biol.* **2016**, *99*, 955–969. [[CrossRef](#)] [[PubMed](#)]
99. Ludwig, A.; Schiemann, F.; Mentlein, R.; Lindner, B.; Brandt, E. Dipeptidyl peptidase IV (CD26) on T cells cleaves the CXC chemokine CXCL11 (I-TAC) and abolishes the stimulating but not the desensitizing potential of the chemokine. *J. Leukoc. Biol.* **2002**, *72*, 183–191. [[PubMed](#)]
100. Lambeir, A.-M.; Durinx, C.; Scharpé, S.; De Meester, I. Dipeptidyl-Peptidase IV from Bench to Bedside: An Update on Structural Properties, Functions, and Clinical Aspects of the Enzyme DPP IV. *Crit. Rev. Clin. Lab. Sci.* **2003**, *40*, 209–294. [[CrossRef](#)]